

Monomeric Homoleptic (2-Pyridylmethyl)(tert-butyldimethylsilyl)amido Complexes of the Divalent Metals Mg, Mn, Fe, Co, and Zn

Christian Koch^a, Astrid Malassa^a, Christine Agthe^a, Helmar Görls^a, Ralf Biedermann^b, Harald Krautscheid^b, and Matthias Westerhausen^{a,*}

^a Jena, Germany, Friedrich-Schiller-Universität, Institute of Inorganic and Analytical Chemistry

^b Leipzig, Germany, University, Institute of Inorganic Chemistry

Received November 2nd, 2006.

Abstract. The transamination reaction of $M[N(\text{SiMe}_3)_2]_2$ with (2-pyridylmethyl)(tert-butyldimethylsilyl)amine yields the corresponding homoleptic metal bis[(2-pyridylmethyl)(tert-butyldimethylsilyl)amides] of Mg (**1**), Mn (**2**), Fe (**3**), Co (**4**) and Zn (**5**). All these compounds crystallize from hexane isotypic in the space group $C2/c$. From toluene the zinc derivative precipitates as toluene solvate **5**·toluene. The molecular structures of these compounds are very similar with large NMN angles to the amide nitrogen atoms with NMN values of 148° (**1**) and 150° (**5**) for the diamagnetic compounds and 156° for the paramagnetic derivatives **2** and **3**. The Co derivative **4** displays a rather small NCoN angle of 142° . Different synthetic routes have been explored for compound **3** which is also available via the metallation reaction of bis(2,4,6-trimethyl-

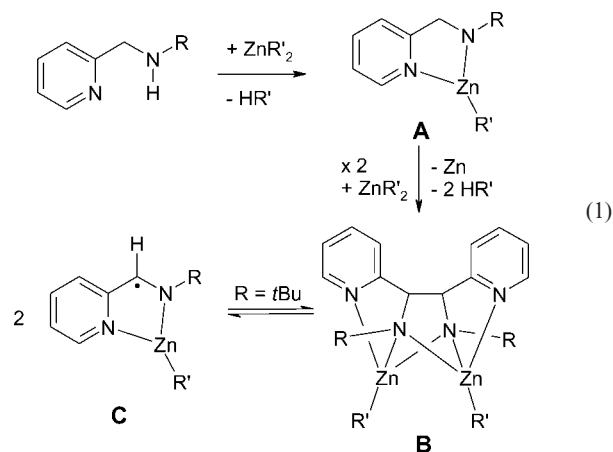
phenyl)iron with (2-pyridylmethyl)(tert-butyldimethylsilyl)amine and via the metathesis reaction of lithium (2-pyridylmethyl)(tert-butyldimethylsilyl)amide with $[(\text{thf})_2\text{FeCl}_2]$. In course of the metathesis reaction, an equimolar amount of lithium (2-pyridylmethyl)(tert-butyldimethylsilyl)amide and $[(\text{thf})_2\text{FeCl}_2]$ yields heteroleptic (2-pyridylmethyl)(tert-butyldimethylsilyl)amido iron(II) chloride (**6**) which crystallizes as a centrosymmetric dimeric molecule. The oxidative C-C coupling reaction of **5** with $\text{Sn}[N(\text{SiMe}_3)_2]_2$ leads to the formation of tin(II) 1,2-bis(2-pyridyl)-1,2-bis(tert-butyldimethylsilylamido)ethane, tin metal and $\text{Zn}[N(\text{SiMe}_3)_2]_2$.

Keywords: Amides; C-C Coupling reactions; Homoleptic complexes; Metallation reactions; Transamination reactions

Introduction

2-Pyridylmethylamines are easily deprotonated at the amine unit by dialkylzinc to give compound **A** according to equation (1) [1]. However, at elevated temperatures an oxidative C-C coupling reaction is observed yielding bis(alkylzinc) 1,2-bis(2-pyridyl)-1,2-bis(amido)ethane (**B**) [1, 2]. Depending on the substituent R at the amide nitrogen atom, an equilibrium of this complex with its dissociation product **C** forms for $R = t\text{Bu}$ via a homolytic C-C bond cleavage [3–5]. If R resembles a trialkylsilyl ligand no C-C bond cleavage is detected [2].

Regardless of the stoichiometry of the first metallation step, only heteroleptic compounds **A** are obtained, the synthesis of homoleptic zinc bis(2-pyridylmethylamide)s fails. The unwillingness of the $R'\text{Zn}$ moieties in alkylzinc amides to undergo metallation reactions was observed earlier also with smaller amide ligands [6, 7]. Also in the dinuclear complex **B** the alkyl substituents R' show an extreme low reactivity [8]. Therefore, alterations at the metal atom are hard

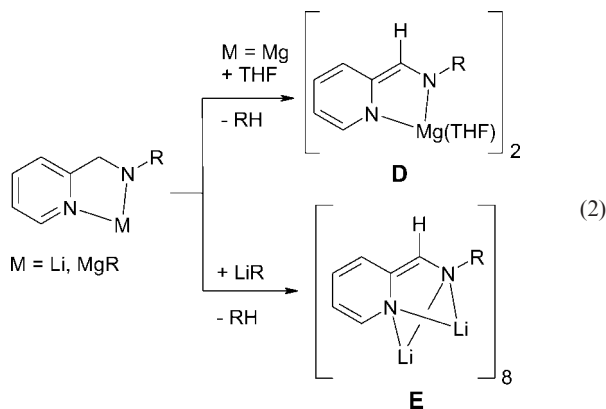


to perform and a different pathway has to be found in order to prepare the homoleptic complexes.

The second C-C coupling step strongly depends on the standard potential $E^0(M/M^{2+})$ of the metal M. Whereas the reaction of $\text{Sn}[N(\text{SiMe}_3)_2]_2$ [$E^0(\text{Sn}/\text{Sn}^{2+}) = -0.14 \text{ V}$] with (2-pyridylmethyl)(tert-butyldimethylsilyl)amine gives the corresponding C-C coupling reaction already at room temperature, elevated temperatures are necessary for the similar reaction with dialkylzinc [$E^0(\text{Zn}/\text{Zn}^{2+}) = -0.76 \text{ V}$] [1, 2]. The reaction mechanism is not yet fully understood, however, the initial reaction is the intramolecular deprotonation of the methylene moiety under loss of the aromatic character of the pyridyl fragment according to equation (2) thus

* Prof. Dr. M. Westerhausen
Institut für Anorgan. und Analyt. Chemie
Friedrich-Schiller-Universität
August-Bebel-Str. 2
D-07743 Jena
Fax: +49 (0) 3641 948110
e-mail: m.we@uni-jena.de

giving a bisamide species. This divalent anion was isolated as a dimeric magnesium (**D**) [2] [$E^0(\text{Mg}/\text{Mg}^{2+}) = -2.36 \text{ V}$] and as an octameric lithium derivative (**E**) [9] [$E^0(\text{Li}/\text{Li}^+) = -3.04 \text{ V}$] because the reduction of these very electropositive metals was impossible in course of a C-C coupling reaction.

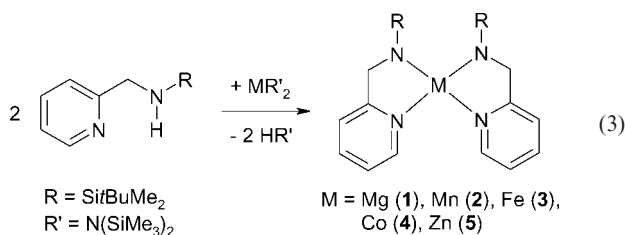


Here we investigate the reaction of (2-pyridylmethyl)(tert-butylidimethylsilyl)amine with the homoleptic bis(trimethylsilyl)amides of the divalent metals Mg, Mn [$E^0(\text{Mn}/\text{Mn}^{2+}) = -1.18 \text{ V}$], Fe [$E^0(\text{Fe}/\text{Fe}^{2+}) = -0.44 \text{ V}$], Co [$E^0(\text{Co}/\text{Co}^{2+}) = -0.28 \text{ V}$], and Zn in order to obtain the homoleptic (2-pyridylmethyl)(tert-butylidimethylsilyl)amides.

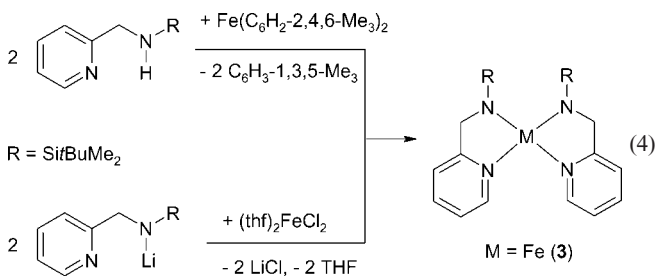
Results and Discussion

Synthesis

Transamination reactions were investigated earlier with support of theoretical considerations [10]. In a similar procedure, the employment of zinc bis[bis(trimethylsilyl)amide] [11] allows the synthesis of zinc bis[(2-pyridylmethyl)(tert-butylidimethylsilyl)amide] (**5**) with high yield according to equation (3). An excess of amine does not lead to an enhancement of the coordination number. Addition of dialkylzinc to **5** yields the well-known heteroleptic alkylzinc (2-pyridylmethyl)(tert-butylidimethylsilyl)amide [1, 2]. In order to verify the generality of this synthesis and in order to compare the molecular structures in dependency of the radius and the d-electron count of the metal, (2-pyridylmethyl)(tert-butylidimethylsilyl)amine is deprotonated by the homoleptic bis(trimethylsilyl)amides of magnesium [12, 13], manganese [13–15], iron [16, 17], and cobalt [15, 18] according to equation (3).

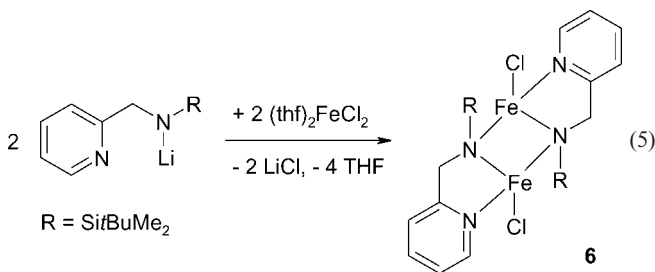


In order to investigate the possibility to employ other synthetic routes for the preparation of the iron complex **3**, bis(2,4,6-trimethylphenyl)iron(II) (dimesityliron) [19] was used as a metallating reagent toward (2-pyridylmethyl)(tert-butylidimethylsilyl)amine. Another access route is the metathesis reaction of $[(\text{thf})_2\text{FeCl}_2]$ with lithium (2-pyridylmethyl)(tert-butylidimethylsilyl)amide according to equation (4). The paramagnetic compounds **2**, **3** and **4** ($M = \text{Mn}$, Fe , Co) are extremely air and moisture sensitive, far more than the diamagnetic complexes **1** and **5** ($M = \text{Mg}$, Zn).



For all preparative procedures of **3** the yields are rather low. Compound **3** is hard to crystallize and the addition of small amounts of TMEDA or DME can initiate the crystallization process, even though no TMEDA or DME adducts are observed. The crystals of **2**, **3** and **4** often are covered with dark oil and repeated recrystallization procedures from hydrocarbons are necessary and lead to a decrease of the yield.

The metathesis reaction of $[(\text{thf})_2\text{FeCl}_2]$ with lithium (2-pyridylmethyl)(tert-butylidimethylsilyl)amide proceeds stepwise and therefore the isolation of (2-pyridylmethyl)(tert-butylidimethylsilyl)amido iron(II)chloride (**6**) is possible according to equation (5). This heteroleptic iron complex **6** dimerizes and precipitates in the shape of pale yellow needles. An excess of lithium (2-pyridylmethyl)(tert-butylidimethylsilyl)amide yields the homoleptic derivative **3**.



The similarity of the molecular structures of **1** to **5** is supported by mass spectrometric investigations. These derivatives show a very intense M^+ signal besides $[\text{M}-\text{Bu}]^+$. A weaker mass signal was detected for $[\text{M}-\text{Me}]^+$. All of these signals show the isotopic pattern of silicon and the metals. In addition, the IR spectra are also very similar and support the conclusion that the bis(amides) of Mg, Mn, Fe, Co, and Zn precipitate with very similar molecular structures.

Molecular Structures

The compounds **1** to **5** crystallize isotypic and a comparison of the structural parameters is given in Table 1, for comparison reasons (2-pyridylmethyl)(tert-butyldimethylsilyl)amine is included as a complex at dimeric LiI [20]. As representative examples, Figures 1 and 2 show the molecular structures of **3** and **5**, whereas a superposition of **2** and **4** is displayed in Figure 3.

Table 1 Comparison of selected bond lengths (average values, pm) and angles $^\circ$ of the homoleptic complexes **1** to **5**. The radii $r(M^{2+})$ (pm) refer to tetrahedrally coordinated metal cations, the metal radii $r(M_{\text{metal}})$ refer to the metal structures with twelve-coordinate metal atoms.

	[Li:L] ₂ ^{a)}	Mg (1)	Mn (2)	Fe (3)	Co (4)	Zn (5)
$r(M^{2+})$	73 (Li ⁺)	71	80	77	72	74
$r(M_{\text{metal}})$	157	160	137	126	125	134
M-N2	213.6(5)	198.9(2)	202.9(5)	196.1(2)	192.9(2)	192.6(2)
M-N1	202.4(5)	213.4(2)	221.0(5)	212.3(2)	206.6(2)	211.7(2)
N2-M-N2'	—	148.2(2)	155.7(3)	155.5(1)	141.9(1)	149.95(7)
N2-M-N1	83.6(2)	82.65(9)	80.2(2)	82.21(6)	84.16(6)	83.84(7)
N2-M-N1'	—	114.6(1)	113.5(2)	111.79(6)	115.19(7)	113.48(7)
N1-M-N1'	—	116.4(1)	113.8(3)	112.54(8)	120.51(9)	111.71(7)
N2-Si	177.3(2)	169.5(2)	169.3(5)	170.3(2)	169.7(2)	170.4(2)
N2-C6	146.5(3)	144.9(4)	144.0(7)	145.3(2)	144.9(2)	144.6(3)
N1-C1	133.5(4)	133.3(4)	134.0(7)	134.7(2)	134.0(3)	135.0(3)
N1-C5	133.6(3)	134.5(4)	132.9(7)	133.8(2)	134.1(2)	133.2(3)
C1-C2	137.4(5)	137.2(4)	138.2(9)	137.2(3)	137.2(3)	137.1(3)
C2-C3	136.9(5)	137.8(5)	136.4(9)	138.8(3)	138.1(4)	139.6(3)
C3-C4	137.4(5)	136.7(4)	139.3(8)	137.5(3)	136.7(4)	138.6(3)
C4-C5	138.5(4)	139.0(4)	138.4(8)	139.4(3)	139.2(3)	139.8(3)
C5-C6	150.3(4)	151.3(4)	150.6(8)	150.4(3)	149.2(3)	151.5(3)
M-N2-Si	123.7(2)	125.6(1)	123.4(3)	124.12(9)	123.74(8)	124.90(9)
M-N2-C6	103.8(2)	114.0(2)	115.0(4)	115.0(1)	113.7(1)	114.2(1)
Si-N2-C6	114.9(2)	120.1(2)	121.5(4)	120.8(1)	122.3(1)	120.3(1)

^{a)} L resembles the neutral bidentate ligand (2-pyridylmethyl)(tert-butyldimethylsilyl)amine at lithium (H2-N2-Li 97(2), H2-N2-Si 107(3), H2-N2-C6 109(3) pm).

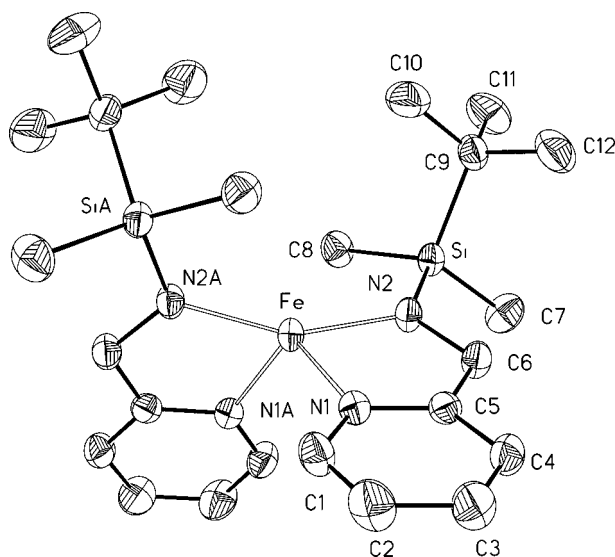


Fig. 1 Molecular structure of iron bis[(2-pyridylmethyl)(tert-butyldimethylsilyl)amido] (**3**). The ellipsoids represent a probability of 40 %, H atoms are omitted for clarity reasons. Symmetry related atoms ($-x, y, -z+0.5$) are marked with "A".

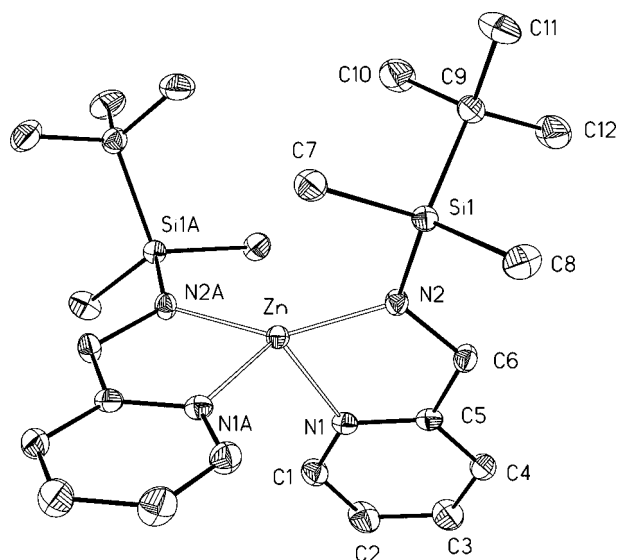


Fig. 2 Molecular structure of zinc bis[(2-pyridylmethyl)(tert-butyldimethylsilyl)amido] (**5**). The ellipsoids represent a probability of 40 %, hydrogen atoms are not shown for clarity reasons. Symmetry related atoms ($-x, y, -z+0.5$) are marked with "A".

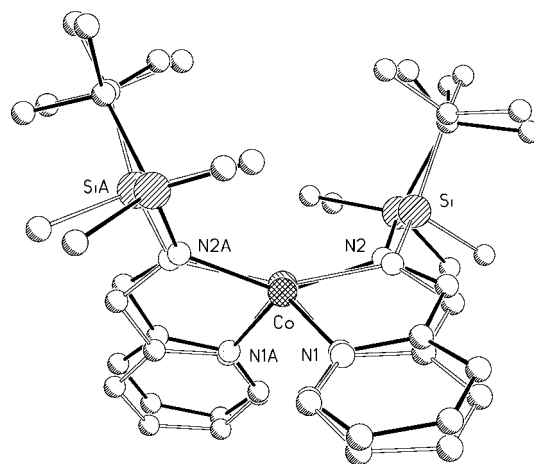


Fig. 3 Superposition of the molecular structures of manganese (**2**) (empty bonds) and cobalt bis[(2-pyridylmethyl)(tert-butyldimethylsilyl)amido] (**4**) (solid bonds). The atoms are drawn with arbitrary radii, H atoms are omitted for clarity reasons. Symmetry related atoms ($-x, y, -z+0.5$) are marked with "A".

The neutral ligand (2-pyridylmethyl)(tert-butyldimethylsilyl)amine, which is coordinated at a lithium cation, shows larger N2-Si and N2-C6 distances than the deprotonated amide ligand of the compounds **1** to **5**. The smaller N2-C6 bond of the amide substituent is a consequence of the larger s-orbital participation of the planarily coordinated N2 atom. The shortening of the N2-Si bond after deprotonation is much more significant and has several reasons: (i) larger s-orbital participation of the sp^2 -hybridized N2 atom, (ii) enhanced electrostatic attraction between the negative N2 and the partly positive silicon atom and (iii)

backdonation from the $p_z(\text{N})$ lone pair into a $\sigma^*(\text{Si}-\text{C})$ orbital.

The complexes **1** to **5** display $\text{N}2-\text{M}-\text{N}2'$ angles between 142° (**1**) and 156° (**2**). The coordination sphere lies between a distorted tetrahedron and a linear arrangement with two additional loose contacts to the pyridyl units. Derivative **1** ($\text{M} = \text{Mg}$, d^0 system) and the Zn compound **5** (d^{10} system) are very much alike, even though Mg usually prefers a tetrahedral and Zn often a linear coordination sphere. This observation can be interpreted that the ligands play the key role and perform a coordination gap which can be filled by any metal ions of the appropriate size and that the electronic state of the $3d$ orbitals is of minor importance.

In order to verify this interpretation, paramagnetic complexes are isolated for Mn (**2**, d^5), Fe (**3**, d^6) and Co (**4**, d^7). The paramagnetic compounds **2** and **3** display larger $\text{N}2-\text{M}-\text{N}2'$ angles than the Mg and Zn derivatives. This observation can be explained by involvement of the partly filled d -orbitals in the σ -bonding situation. A linearization would maximize the orbital interactions between the ligand and the metal center. However, any kind of a π -bond between the nitrogen lone pair and the metal atom can be excluded because this interaction should lead to an increase of the $\text{N}2-\text{Si}$ bond which has not been found. The cobalt derivative **4** displays the smallest $\text{N}2-\text{M}-\text{N}2'$ angle of these compounds. Cobalt is the smallest metal atom of our examples and therefore, the intramolecular steric strain induced by the bulky trialkylsilyl groups is enhanced which leads to a distortion towards a tetrahedron. Whereas the derivatives of Mg , Mn , Fe , and Zn are very much alike, the deviation of the cobalt-containing compound is displayed in Figure 3 as a superposition of **2** and **4**.

A comparison of **1** to **5** with $\text{M}[\text{N}(\text{SiMe}_3)_2]_2$ and its dimers is given in Table 2 and shows that the $\text{M}-\text{N}2$ bond lengths compare fairly well with the terminal distances of the dimeric molecules with three-coordinate metal atoms. In comparison to the monomeric molecules expectedly an elongation of the $\text{M}-\text{N}$ bond is observed. In the solid state monomeric molecules are found for zinc bis[bis(trimethylsilyl)amide] and therefore no comparison data can be given. However, anionic tris[bis(trimethylsilyl)amino]zincates are known and display $\text{Zn}-\text{N}$ values of 197 pm [24]. The manganese derivatives display the largest bond lengths as can be expected for high spin complexes. Andersen et al. [16]

Table 2 Comparison of $\text{M}-\text{N}$ bond lengths in compounds with the metals $\text{M} = \text{Mg}$, Mn , Fe , Co , and Fe in dependency of the coordination number $\text{C.N.}(\text{M})$ of the metal M .

M	1 – 5	M[N(SiMe ₃) ₂] ₂		{(Me ₃ Si) ₂ N _t -M[μ-N _{br} (SiMe ₃) ₂] ₂		
	M-N ₂ /pm	Method ^{a)}	M-N/pm	Method ^{a)}	M-N _t /pm	M-N _{br} /pm
Mg	198.8	GED [21]	191	X-ray [22]	198	215
Mn	202.9	GED [16]	195	X-ray [15]	200	217
Fe	196.1	GED [16]	184	X-ray [17]	193	208
Co	192.9	GED [16]	184	X-ray [15]	192	206
Zn	192.6	X-ray [23]	183			

^{a)} Electron diffraction at the gaseous phase (GED), X-ray structure determination at a single crystal (X-ray).

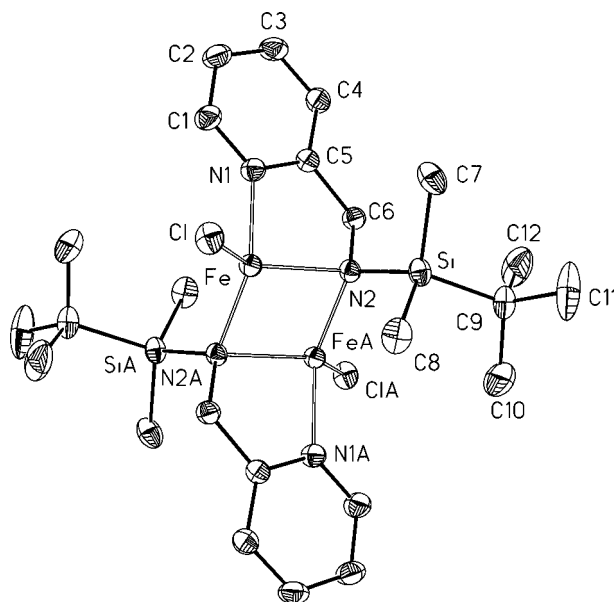


Fig. 4 Molecular structure of the centrosymmetric (2-pyridylmethyl)(tert-butyl dimethylsilyl)amido iron(II) chloride dimer (**6**). Symmetry related atoms ($-x+1$, $-y$, $-z+2$) are marked with "A". The ellipsoids represent a probability of 40 %, hydrogen atoms are neglected for clarity reasons. Selected bond lengths /pm:

$\text{Fe}-\text{N}1$ 208.0(2), $\text{Fe}-\text{N}2$ 210.7(2), $\text{Fe}-\text{N}2'$ 201.2(2), $\text{Fe}-\text{Cl}$ 226.18(7), $\text{N}2-\text{Si}$ 175.5(2), $\text{N}2-\text{C}6$ 148.7(3), $\text{Fe}\cdots\text{Fe}'$ 273.63(7); angles ($^\circ$): $\text{N}1-\text{Fe}-\text{Cl}$ 102.31(6), $\text{N}1-\text{Fe}-\text{N}2$ 81.82(8), $\text{N}1-\text{Fe}-\text{N}2'$ 128.60(8), $\text{N}2-\text{Fe}-\text{Cl}$ 131.31(6), $\text{Cl}-\text{Fe}-\text{N}2'$ 115.31(6), $\text{N}2-\text{Fe}-\text{N}2'$ 96.76(7).

showed that even monomeric $\text{Mn}[\text{N}(\text{SiMe}_3)_2]_2$ is high spin what most probably is also the case for the isostructural iron derivative. The fact that the $\text{M}-\text{N}$ bond lengths are in accordance with the $\text{M}-\text{N}_t$ distances of dimeric $\text{M}[\text{N}(\text{SiMe}_3)_2]_2$ support the interpretation that the compounds **1** to **5** show a coordination behaviour between a tetrahedron and a linear arrangement.

The crystallization behaviour of **3** can be favoured by the addition of small amounts of TMEDA or DME. The formation of an adduct was not observed. This fact demonstrates the effective shielding of the metal center by the (2-pyridylmethyl)(tert-butyl dimethylsilyl)amide anions. Lee et al. [25] showed that TMEDA can serve as a base with a flexible coordination behaviour. Thus, TMEDA can bind in a monodentate or a bidentate as well as in a bridging fashion. In the heteroleptic complexes $[(\text{TMEDA})\text{FeL}_2]$ with L as a bulky bidentate benzamidinate ligand the iron atom is penta-coordinated. In $[\text{L}_2\text{Mn}(\mu\text{-TMEDA})\text{MnL}_2]$ the TMEDA molecule acts as a N,N' -bridging Lewis base. Homoleptic compounds with bulky azaallyl substituents of iron(II) show a favoured η^3 -coordination, however, extreme bulkiness leads to a two-coordinate iron center with a bent $\text{N}-\text{Fe}-\text{N}$ unit [26]. In the compounds **2** and **3** Lewis bases such as ethers or amines are unable to form complexes due to steric reasons. However, small molecules such as oxygen or water react immediately with these derivatives which explains the extreme sensitivity towards air and moisture.

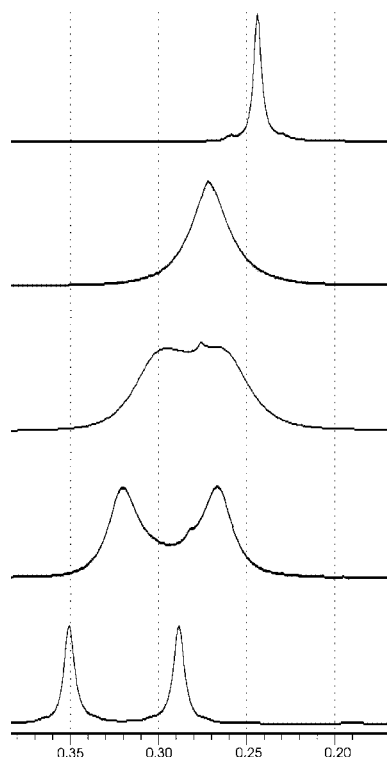


Fig. 5 DNMR studies of compound **5** (solvent: $[D_8]$ toluene). Only the 1H -NMR spectra of the resonances of the silicon-bound methyl groups are shown at various temperatures at 345 K, 318 K, 308 K, 300 K, and 280 K (from the top to the bottom spectrum).

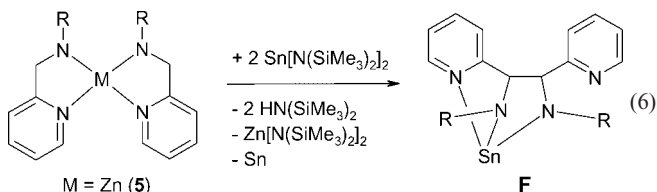
The molecular structure and numbering scheme of the centrosymmetric (2-pyridylmethyl)(tert-butyldimethylsilyl)amido iron(II)chloride dimer (**6**) is displayed in Figure 4. The structural parameters differ from those of the homoleptic derivative **3** due to the coordination number of four for the amide nitrogen atom N2. Due to this fact the N2 atom is in a distorted tetrahedral environment and therefore the back donation of charge from the $p_z(N)$ orbital into the $\sigma^*(Si-C)$ orbital is not possible. Consequently, the N2-Si bond length increases significantly and shows a value of 175.5(2) pm. The lower s-orbital participation in the Fe-N bond also leads to an elongation of the Fe-N2 distances.

DNMR studies

Due to the paramagnetism of the coordination compounds of Mn (**2**), Fe (**3**) and Co (**4**), NMR studies were only possible with the diamagnetic magnesium (**1**) and zinc complexes (**5**). At room temperature the resonance of the silicon-bound methyl groups of **1** and **5** are broadened. Temperature-dependent NMR studies show that the chemical shift is temperature-dependent and that the signal becomes narrow at high temperatures and splits into two resonances at low temperatures as shown in Figure 5. This dynamic behaviour results from a hindered rotation of the tert-butyldimethylsilyl group around the Si-N bond. With the Gutowsky-Holm equation the exact determination of the

rotation barrier is possible based on the coalescence temperature ($T_c = 285$ K for **1** and $T_c = 310$ K for **5** at 200.129 MHz) and the line separation at low temperatures ($\Delta\delta = 10.5$ Hz for **1** and $\Delta\delta = 12.4$ Hz for **5**). With these data rotation barriers of 67.4 and 62.1 $\text{kJ}\cdot\text{mol}^{-1}$, respectively, have been estimated for the Mg (**1**) and Zn (**5**) compounds. The slight difference of 5.3 $\text{kJ}\cdot\text{mol}^{-1}$ is in agreement with the results of the X-ray structures: The slight elongation of the metal-nitrogen bonds in the magnesium derivative **1** leads to decreasing steric strain and consequently to a smaller rotation barrier around the Si-N bond of the tert-butyldimethylsilyl substituent.

Reactivity studies. Even though the metal centers of the complexes **1** to **5** are shielded quite effectively by the bulky ligands, reactions at the periphery should be possible. These (2-pyridylmethyl)(tert-butyldimethylsilyl)amide substituents offer the possibility to form a C-C bond by a metal mediated oxidation reaction similar to the reaction shown in equation (1). As a representative example, the diamagnetic zinc derivative **5** was reacted with tin(II) bis[bis(trimethylsilyl)amide] allowing a NMR spectroscopic characterization of the products. In accordance to the expected reaction pathway we observed the C-C coupling product and the formation of metal powder. X-ray diffraction experiments showed that only tin metal precipitated. However, the tin(II) derivative does not only initiate a C-C coupling reaction, but also a metal-metal exchange reaction (transamination). Thus, the already well-known mononuclear tin(II) 1,2-bis(2-pyridyl)-1,2-bis(tert-butyldimethylsilylamido)-ethane [**1**, **2**] was isolated according to equation (6). Simultaneously $Zn[N(SiMe_3)_2]_2$ was formed, because the newly formed C-C bond leads to an opening of the coordination sphere at zinc, thus enabling this transamination step.



The reaction of the iron compound **3** with $Sn[N(SiMe_3)_2]_2$ also led to the precipitation of metal powders. However, a powder diffractogram confirmed that iron and tin were formed simultaneously. The solution was decanted and all volatile materials were removed under vacuum. Mass spectrometric investigations of the residue confirmed the formation of the C-C coupled ligand. However, an isolation of a metal complex with the C-C coupled tetradentate ligand from the oily residue failed thus far.

It was not possible to isolate bis[(2-pyridylmethyl)(tert-butyldimethylsilyl)amido]iron(III) chloride from the metathesis reaction of lithium (2-pyridylmethyl)(tert-butyldimethylsilyl)amide with $FeCl_3$. Instead of an iron(III) complex, compound **6** was obtained with a yield of 17 %. Mass spectrometric investigations showed that C-C coupling reactions have occurred. This observation is plausible regarding the standard potential $E^0(Fe^{2+}/Fe^{3+})$ of +0.77 V. Al-

ready thirty years ago also *Bradley* and *Chisholm* [27] noticed that dialkylamides of iron(III) are not stable but they form C-C coupling products.

The rather low yields of **3** and **4** can also be understood by partial subsequent formation of C-C coupling products during the transamination reaction. The raw materials of **3** and **4** were covered with an oily substance after the common work-up procedures and had to be recrystallized. The comparison of the standard potentials of Sn [$E^0(\text{Sn}/\text{Sn}^{2+}) = -0.14 \text{ V}$] with Mg [$E^0(\text{Mg}/\text{Mg}^{2+}) = -2.36 \text{ V}$], Mn [$E^0(\text{Mn}/\text{Mn}^{2+}) = -1.18 \text{ V}$], Fe [$E^0(\text{Fe}/\text{Fe}^{2+}) = -0.44 \text{ V}$], Co [$E^0(\text{Co}/\text{Co}^{2+}) = -0.28 \text{ V}$] and Zn [$E^0(\text{Zn}/\text{Zn}^{2+}) = -0.76 \text{ V}$] explains why for the paramagnetic complexes **3** and **4** C-C coupling side reactions occur whereas for magnesium only transamination reactions have to be considered.

Summary and Perspectives

The synthesis of homoleptic metal bis[(2-pyridylmethyl)(tri-alkylsilyl)amides] of Mg, Mn, Fe, Co, and Zn succeeds via a transamination reaction. Due to similar radii of these metal cations between 70 and 80 pm, these compounds crystallize isotypic with strongly widened NMN bond angles. These isotypic structures suggest that the packing of the ligands preforms the coordination gap which is occupied by the metal atom. The steric shielding allows the synthesis of homoleptic alkylamides even of the paramagnetic metal cations manganese, iron and cobalt.

The open shell systems (paramagnetic complexes) are much more sensitive towards moisture and air than the diamagnetic compounds of Mg and Zn. The addition of $\text{Sn}[\text{N}(\text{SiMe}_3)_2]_2$ leads to a C-C coupling reaction, however, also transamination reactions take place. Therefore, no analytically pure product with a C-C coupled tetradentate 1,2-bis(2-pyridyl)-1,2-bis(tert-butyldimethylsilylamido)ethane ligand of Mg, Mn, Fe, Co, or Zn was available from this reaction as of yet.

Experimental Part

General procedure: All manipulations were carried out in an anhydrous argon atmosphere and the solvents were thoroughly dried. Starting $\text{M}[\text{N}(\text{SiMe}_3)_2]_2$ with $\text{M} = \text{Mg}, \text{Mn}, \text{Fe}, \text{Co}$, and Zn as well as FeMe_2 were prepared according to literature procedures. The N and C values of the elemental analysis are too small due to nitride and carbonate formation during combustion.

Synthesis of magnesium bis[(2-pyridylmethyl)(tert-butyldimethylsilyl)-amide] (1). 1,1,1,3,3,3-Hexamethyldisilazane (0.97 g, 6.01 mmol) was dissolved in 4 mL of toluene. Dibutylmagnesium dissolved in toluene (3 mL of a 1.0 molar solution) was added at r.t. After complete addition the reaction mixture was heated to 40 °C and the evolution of butane was observed for the next 2 h. Thereafter (2-pyridylmethyl)(tert-butyldimethylsilyl)amine (0.68 g, 3.06 mmol) was added and the initially light yellow solution turned brown to purple. The volatile materials were removed under vacuum. The residue was dissolved in n-hexane. Storage of this solution for one

week at -10°C led to the precipitation of colorless crystals. Yield: 1.33 g (2.85 mmol, 95 %). Elemental analysis ($\text{C}_{24}\text{H}_{42}\text{MgN}_4\text{Si}_2$, 467.11): calcd. C 61.71, H 9.06, N 11.99; found: C 60.09, H 9.06, N 11.60 %. M.p. 136 °C (dec.).

^1H NMR (C_6D_6): $\delta = 7.91 - 7.89$ (d, H1), 6.91 – 6.83 (m, H3), 6.69 – 6.66 (d, H4), 6.43 – 6.37 (m, H2), 4.91 (s, H6), 1.29 (s, CCH₃), 0.29 (s, SiCH₃). **$^{13}\text{C}\{^1\text{H}\}$ NMR** (C_6D_6): $\delta = 170.4$ (C5), 146.4 (C1), 138.7 (C3), 122.6 (C2), 121.1 (C4), 54.3 (C6), 28.4 (CCH₃), 20.9 (CCH₃), –3.27 and –3.39 (SiCH₃). **IR** (Nujol, KBr, cm^{-1}): 1590 s, 1570 s, 1462 s, 1377 s, 1251 s, 1121 s, 935 m, 830 s, 775 s, 662 m, 628 w.

Synthesis of manganese bis[(2-pyridylmethyl)(tert-butyldimethylsilyl)amide] (2). $\text{Mn}[\text{N}(\text{SiMe}_3)_2]_2$ (0.375 g, 1.0 mmol) was dissolved in 10 mL of hexane. At r.t. 0.222 g of (2-pyridylmethyl)(tert-butyldimethylsilyl)amine (1.0 mmol) was added dropwise. The pink solution turned purple immediately. All solid material was removed. At r.t. yellow crystals precipitated within several hours. This compound is extremely sensitive towards air and moisture. Upon isolation the crystals liquefied and turned into a brown oily substance. Therefore the determination of the melting point gave no reproducible results. The yield was approximately 20 %. Elemental analysis ($\text{C}_{24}\text{H}_{42}\text{MnN}_4\text{Si}_2$, 497.74): calcd. C 57.92, H 8.51, N 11.26; found: C 58.00, H 8.18, N 11.21 %.

EPR (298 K): $g = 2.0298$. **IR** (Nujol, KBr, cm^{-1}): 1592 m, 1570 m, 1462 vs, 1406 m, 1377 s, 1252 s, 1124 s, 1047 w, 1006 w, 830 vs, 769 s, 662 m. **MS** (DEI, m/z): 497 (M^+ , 100 %), 482 ($[\text{M-Me}]^+$, 8 %), 440 ($[\text{M-Bu}]^+$, 69 %).

Synthesis of iron bis[(2-pyridylmethyl)(tert-butyldimethylsilyl)-amide] (3). Method A: (2-Pyridylmethyl)(tert-butyldimethylsilyl)amine (0.222 g, 1.0 mmol) was added dropwise at -20°C to a solution of 0.376 g of $\text{Fe}[\text{N}(\text{SiMe}_3)_2]_2$ (1.0 mmol). During the addition the green solution darkens immediately. After complete addition the reaction mixture was filtered and the solution cooled to -20°C . Slightly yellow single crystals precipitated from this dark green mother liquor. After isolation and during drying the crystals liquefied and turned into a dark oily substance. If the crystallization failed all volatile materials were removed in vacuum till an oily residue remained. Then addition of a small amount of DME or TMEDA and cooling to -20°C led to the precipitation of crystals of **3**.

Method B: To a suspension of 0.26 g of dimesityliron(II) (0.9 mmol) in 7 mL of diethylether, a solution of (2-pyridylmethyl)(tert-butyldimethylsilyl)amine in 5 mL of Et_2O was added at -78°C . After warming to r.t. the red-brown solution was filtered and then all volatile materials were removed. The red-brown residue was redissolved in boiling THF. Slow cooling to -20°C led to the precipitation of colorless crystals of **3** covered with red oil.

Method C: At -78°C 1.4 mL of a 1.6M BuLi solution in hexane were dropped to a solution of 0.5 g of (2-pyridylmethyl)(tert-butyldimethylsilyl)amine (2.2 mmol) in 5 mL of THF. This solution was added dropwise at -78°C to a suspension of 0.26 g of $(\text{thf})_2\text{FeCl}_2$ in 5 mL of THF. After complete addition the red-brown reaction mixture was slowly warmed to r.t. After removal of all volatile materials the residue was dissolved in 10 mL of pentane. After filtration 0.10 g of colorless crystals of **3** (0.2 mmol, 18 %) precipitated at -20°C . Elemental analysis ($\text{C}_{24}\text{H}_{42}\text{FeN}_4\text{Si}_2$, 498.65): calc.: C 57.81, H 8.49, N 11.24; found: C 57.12, H 8.97, N 9.69 %. M.p. 58 °C (dec.).

IR (nujol, KBr, cm^{-1}): 1602 m, 1568 w, 1480 m, 1278 w, 1241 s, 1152 w, 1054 m, 1037 s, 1003 vs, 956 m, 826 vs, 772 s, 762 s, 661 m, 631 m, 516 m. **MS** (DEI, m/z): 498 (M^+ , 93 %), 483 ($[\text{M-Me}]^+$, 22 %), 441 ($[\text{M-Bu}]^+$, 100 %), 223 (18 %).

Synthesis of cobalt bis[(2-pyridylmethyl)(tert-butyldimethylsilyl)-amide] (4). At r.t. 0.44 g of (2-pyridylmethyl)(tert-butyldimethylsilyl)amine (2.0 mmol) was added to 0.76 g of cobalt bis[bis(trimethylsilyl)amide] (2.0 mmol) in 10 mL of hexane. After complete addition all solids were removed from this dark green solution by filtration. Cooling to -18°C afforded the precipitation of dark brown crystals of **4**. After isolation the crystals slowly liquefied and decomposed. Therefore, no melting point can be given. Elemental analysis ($\text{C}_{24}\text{H}_{42}\text{MnN}_4\text{Si}_2$, 501.73): calcd.: C 57.45, H 8.44, N 11.17; found: C 56.02, H 8.40, N 10.77 %.

IR (Nujol, KBr, cm^{-1}): 1592 m, 1570 w, 1463 vs, 1405 m, 1378 m, 1251 s, 1122 s, 1046 w, 1006 w, 937 w, 890 w, 830 vs, 772 m, 762 m, 753 m, 661 m. **MS** (DEI, m/z): 501 (M^+ , 100 %), 486 ($[\text{M}-\text{Me}]^+$, 12 %), 444 ($[\text{M}-\text{Bu}]^+$, 94 %), 223 (4 %), 163 (18 %).

Synthesis of zinc bis[(2-pyridylmethyl)(tert-butyldimethylsilyl)-amide] (5). A solution of 1.79 g of (2-pyridylmethyl)(tert-butyldimethylsilyl)amine (8.05 mmol) in 5 mL of toluene or hexane was stirred at r.t. Then a solution of 1.56 g of $\text{Zn}[\text{N}(\text{SiMe}_3)_2]_2$ (4.04 mmol) was added dropwise. After stirring over night a small amount of colorless precipitate formed and was removed. The volume of the solution was reduced to 2/3 of the original volume. After 3 d at r.t. colorless crystals of **5** were collected. After reduction of the volume of the mother liquor another crop of crystals was isolated. The solid material was dissolved in 10 mL of toluene. After 2 weeks at -10°C colorless crystals of **5**·1/2 toluene (M.p. 75°C) were isolated. Recrystallization from hexane gave 1.83 g of solvent-free crystalline **5** (3.60 mmol, 90 %). M.p. 110°C . Elemental analysis ($\text{C}_{24}\text{H}_{42}\text{N}_4\text{Si}_2\text{Zn}$, 508.17): Calcd. C 56.73, H 8.33, N 11.03, found: C 56.01, H 8.22, N 10.87 %.

^1H NMR (C_6D_6): δ = 7.96 – 7.93 (d, H1), 6.94 – 6.86 (m, H3), 6.69 – 6.65 (d, H4), 6.46 – 6.40 (m, H2), 4.93 (s, H6), 1.23 (s, CCH_3), 0.27 (s, SiCH_3). **$^{13}\text{C}\{^1\text{H}\}$ NMR** (C_6D_6): δ = 166.6 (C5), 149.2 (C1), 136.9 (C3), 122.3 (C2), 121.4 (C4), 54.6 (C6), 28.3 (CCH_3), 21.6 (CCH_3), -3.02 and -2.87 (SiCH_3).

IR (Nujol, KBr, cm^{-1}): 3371 w, 2925 s, 2854 s, 1592 s, 1570 s, 1463 s, 1377 s, 1252 s, 1124 s, 937 m, 830 s, 776 s, 662 m, 628 w, 593 w. **MS** (EI): 508 (M^+ , 8 %). **MS** (DEI, m/z): 506 (M^+ , 16 %), 491 ($[\text{M}-\text{Me}]^+$, 3 %), 449 ($[\text{M}-\text{Bu}]^+$, 100 %), 163 (95 %).

Synthesis of (2-pyridylmethyl)(tert-butyldimethylsilyl)amido iron(II)chloride (6). At -78°C a solution of *n*BuLi in hexane (1.6M, 1.0 mL) was added to 0.36 g of 2-pyridylmethylamine (1.6 mmol) in 5 mL of THF. After 5 minutes of stirring and warming to r.t. this solution was dropped at -78°C to a suspension of 0.38 g of $(\text{thf})_{1.5}\text{FeCl}_2$ in 5 mL of THF. The reaction mixture turned red immediately. During the warm-up after complete addition the solution changed its color to yellow-brown. At r.t. the solution was allowed to stand without stirring. During 17 h a pale yellow powder precipitated. Reduction of the volume of the mother liquor and cooling to 5°C gave another crop of **6**. Yield: 0.21 g (0.34 mmol; 43 %). M.p. 179°C (dec.). Elemental analysis ($\text{C}_{24}\text{H}_{42}\text{Cl}_2\text{Fe}_2\text{N}_4\text{Si}_2$, 625.71): Calcd. C 46.07, H 6.77, N 8.95, found: C 45.43, H 6.59, N 8.81 %.

IR (Nujol, KBr, cm^{-1}): 1608 m, 1569 w, 1487 m, 1286 w, 1255 m, 1155 w, 1104 w, 1026 m, 991 m, 965 w, 899 w, 823 s, 780 vs, 754 w, 660 m, 638 w, 525 m, 461 w. **MS** (EI): 625 (M^+ , 1 %), 567 ($[\text{M}+\text{Bu}]^+$, 1 %), 498 ($[\text{M}-\text{FeCl}_2]^+$ = 3^+ , 4 %), 165 (100 %).

Structure Determinations. The intensity data of **5** were collected on a Stoe IPDS-2T diffractometer and of **1**, **2**, **3**, **4**, and **5**·toluene on a Nonius Kappa CCD diffractometer using graphite-monochromated Mo- $\text{K}\alpha$ radiation ($\lambda = 0.71073 \text{ \AA}$). Data was corrected for Lorentz polarization and for absorption effects [28–30]. All isotypic compounds **1** to **5** crystallize in the monoclinic space group C2/c . The crystal data and refinement details are summarized in Table 3. The structures were solved by direct methods (SHELXS [31]) and refined by full-matrix least squares techniques against F_o^2 (SHELXL-97 [32]).

Table 3 Crystal data and refinement details for the X-ray structure determinations of the isotypic compounds **1** to **5** as well as **5**·1/2 toluene and **6**.

Compound	1	2	3	4	5	5 ·1/2 toluene	6
formula	$\text{C}_{24}\text{H}_{42}\text{MgN}_4\text{Si}_2$	$\text{C}_{24}\text{H}_{42}\text{MnN}_4\text{Si}_2$	$\text{C}_{24}\text{H}_{42}\text{FeN}_4\text{Si}_2$	$\text{C}_{24}\text{H}_{42}\text{CoN}_4\text{Si}_2$	$\text{C}_{24}\text{H}_{42}\text{N}_4\text{Si}_2\text{Zn}$	$\text{C}_{27.5}\text{H}_{46}\text{N}_4\text{Si}_2\text{Zn}$	$\text{C}_{24}\text{H}_{42}\text{Cl}_2\text{Fe}_2\text{N}_4\text{Si}_2$
fw ($\text{g}\cdot\text{mol}^{-1}$)	467.11	497.74	498.65	501.73	508.17	554.23	625.71
<i>T</i> /K	183(2)	183(2)	183(2)	183(2)	293(2)	183(2)	183(2)
crystal system	monoclinic	monoclinic	monoclinic	monoclinic	monoclinic	triclinic	monoclinic
space group	C2/c (Nr. 15)	C2/c (Nr. 15)	C2/c (Nr. 15)	C2/c (Nr. 15)	C2/c (Nr. 15)	$\text{P}\bar{1}$ (Nr. 2)	$\text{P2}_1/\text{n}$ (Nr. 14)
<i>a</i> /pm	1805.2(2)	1803.21(6)	1786.71(7)	2199.6(1)	1777.6(1)	1053.44(4)	848.81(1)
<i>b</i> /pm	826.12(8)	819.85(3)	823.59(3)	793.36(5)	829.74(8)	1267.38(6)	1740.27(7)
<i>c</i> /pm	2062.3(2)	2074.67(8)	2071.18(8)	2050.1(1)	2050.1(1)	1271.08(6)	1095.03(5)
$\alpha/^\circ$	90	90	90	90	90	82.081(2)	90
$\beta/^\circ$	112.030(6)	111.769(2)	112.016(2)	118.63(3)	112.165(5)	88.955(3)	94.444(3)
$\gamma/^\circ$	90	90	90	90	90	67.221(3)	90
<i>V</i> /Å ³	2850.9(5)	2848.4(2)	2825.5(2)	2832.9(3)	2800.3(4)	1548.6(1)	1612.7(1)
<i>Z</i>	4	4	4	4	4	2	2
$\sigma/\text{g}\cdot\text{cm}^{-3}$	1.088	1.161	1.172	1.176	1.205	1.189	1.288
μ/mm^{-1}	0.164	0.565	0.636	0.707	0.980	0.892	1.158
measured data	9333	9248	9318	9689	9026	10471	6958
data with $I > 2\sigma(I)$	1797	2660	2509	2539	2474	5677	2604
unique data (R_{int})	3194	3252	3240	3225	2740	6847	3698
wR_2 (all data, on F_o^2) ^{a)}	0.1587	0.1026	0.0990	0.0989	0.0937	0.1397	0.0954
R_1 ($I > 2\sigma(I)$) ^{a)}	0.0636	0.0396	0.0383	0.0371	0.0347	0.0509	0.0395
s ^{b)}	1.019	1.024	1.008	1.021	1.089	1.028	1.005
Res. dens./ $\text{e}\cdot\text{\AA}^{-3}$	0.450/-0.241	0.408/-0.479	0.330/-0.372	0.326/-0.337	0.944/-0.739	0.961/-0.530	0.288/-0.459
CCDC No.	CCDC-609814	CCDC-609815	CCDC-609816	CCDC-609817	CCDC-609818	CCDC-609819	CCDC-609820

^{a)} Definition of the *R* indices: $R_1 = (\sum |F_o| - |F_c|) / \sum |F_o|$

$wR_2 = \{\sum [w(F_o^2 - F_c^2)^2] / \sum [w(F_o^2)^2]\}^{1/2}$ with $w^{-1} = \sigma^2(F_o^2) + (aP)^2$.

^{b)} $s = \{\sum [w(F_o^2 - F_c^2)^2] / (N_o - N_p)\}^{1/2}$.

Acknowledgement. This work was supported in the collaborative research initiative of the DFG (SFB 436) and we thank the **Deutsche Forschungsgemeinschaft (DFG, Bonn-Bad Godesberg, Germany)** for generous funding.

Supporting Information available: Crystallographic data (excluding structure factors) has been deposited with the Cambridge Crystallographic Data Centre as supplementary publication CCDC-609814 for **1**, CCDC-609815 for **2**, CCDC-609816 for **3**, CCDC-609817 for **4**, CCDC-609818 for **5**, CCDC-609819 for **5-toluene**, and CCDC-609820 for **6**. Copies of the data can be obtained free of charge on application to CCDC, 12 Union Road, Cambridge CB2 1EZ, UK [E-mail: deposit@ccdc.cam.ac.uk].

References

- [1] M. Westerhausen, T. Bollwein, N. Makropoulos, T. M. Rotter, T. Haberer, M. Suter, H. Nöth, *Eur. J. Inorg. Chem.* **2001**, 851–857.
- [2] M. Westerhausen, T. Bollwein, N. Makropoulos, S. Schneiderbauer, M. Suter, H. Nöth, P. Mayer, H. Piotrowski, K. Polborn, A. Pfizner, *Eur. J. Inorg. Chem.* **2002**, 389–404.
- [3] J. T. B. H. Jastrzebski, J. M. Klerks, G. V. Koten, K. Vrieze, *J. Organomet. Chem.* **1981**, 210, C49–C53.
- [4] G. v. Koten, J. T. B. H. Jastrzebski, K. Vrieze, *J. Organomet. Chem.* **1983**, 250, 49–61.
- [5] E. Wissing, S. v. d. Linden, E. Rijnberg, J. Boersma, W. J. J. Smeets, A. L. Spek, G. v. Koten, *Organometallics* **1994**, 13, 2602–2608.
- [6] M. M. Olmstead, W. J. Grigsby, D. R. Chacon, T. Hascall, P. P. Power, *Inorg. Chim. Acta* **1996**, 251, 273–284.
- [7] M. Westerhausen, T. Bollwein, A. Pfizner, T. Nilges, H.-J. Deiseroth, *Inorg. Chim. Acta* **2001**, 312, 239–244.
- [8] See for example: M. Westerhausen, T. Bollwein, K. Karaghiosoff, S. Schneiderbauer, M. Vogt, H. Nöth, *Organometallics* **2002**, 21, 906–911.
- [9] M. Westerhausen, A. N. Kneifel, N. Makropoulos, *Inorg. Chem. Commun.* **2004**, 7, 990–993.
- [10] D. R. Armstrong, G. C. Forbes, R. E. Mulvey, W. Clegg, D. M. Tooke, *J. Chem. Soc., Dalton Trans.* **2002**, 1656–1661.
- [11] (a) H. Bürger, W. Sawodny, U. Wannagat, *J. Organomet. Chem.* **1965**, 3, 113–120. (b) M. Bochmann, G. Bwembya, K. J. Webb, *Inorg. Synth.* **1997**, 31, 19–23.
- [12] (a) U. Wannagat, H. Kuckertz, *Angew. Chem.* **1963**, 75, 95. (b) M. Westerhausen, *Inorg. Chem.* **1991**, 30, 96–101.
- [13] D. C. Bradley, M. B. Hursthouse, A. A. Ibrahim, K. M. Abdul Malik, M. Motevalli, R. Mösele, H. Powell, J. D. Runnacles, A. C. Sullivan, *Polyhedron* **1990**, 9, 2959–2964.
- [14] (a) H. Bürger, U. Wannagat, *Monatsh. Chem.* **1964**, 95, 1099–1102. (b) B. Horvath, R. Mösele, E. G. Horvath, *Z. Anorg. Allg. Chem.* **1979**, 450, 165–177.
- [15] B. D. Murray, P. P. Power, *Inorg. Chem.* **1984**, 23, 4584–4588.
- [16] R. A. Andersen, K. Faegri, J. C. Green, A. Haaland, M. F. Lappert, W. P. Leung, K. Rypdal, *Inorg. Chem.* **1988**, 27, 1782–1786.
- [17] M. M. Olmstead, P. P. Power, S. C. Shoner, *Inorg. Chem.* **1991**, 30, 2547–2551.
- [18] (a) H. Bürger, U. Wannagat, *Monatsh. Chem.* **1963**, 94, 1007–1012. (b) D. C. Bradley, K. J. Fisher, *J. Am. Chem. Soc.* **1971**, 93, 2058–2059.
- [19] B. Machelett, *Z. Chem.* **1976**, 16, 116–117; see also: H. Müller, W. Seidel, H. Görls, *J. Organomet. Chem.* **1993**, 445, 133–136.
- [20] M. Westerhausen, A. N. Kneifel, P. Mayer, *Z. Anorg. Allg. Chem.* **2006**, 632, 634–638.
- [21] T. Fjeldberg, R. A. Andersen, *J. Mol. Struct.* **1984**, 125, 287–296.
- [22] M. Westerhausen, W. Schwarz, *Z. Anorg. Allg. Chem.* **1992**, 609, 39–44.
- [23] G. Margraf, H.-W. Lerner, M. Bolte, M. Wagner, *Z. Anorg. Allg. Chem.* **2004**, 630, 217–218.
- [24] G. C. Forbes, A. R. Kennedy, R. E. Mulvey, B. A. Roberts, R. B. Rowlings, *Organometallics* **2002**, 21, 5115–5121.
- [25] H. K. Lee, T. S. Lam, C.-K. Lam, H.-W. Li, S. M. Fung, *New J. Chem.* **2003**, 27, 1310–1318.
- [26] A. G. Avent, P. B. Hitchcock, M. F. Lappert, R. Sablong, J. R. Severn, *Organometallics* **2004**, 23, 2591–2600.
- [27] D. C. Bradley, M. H. Chisholm, *Acc. Chem. Res.* **1976**, 9, 273–280.
- [28] COLLECT, Data Collection Software; Nonius B.V., Netherlands, **1998**.
- [29] „Processing of X-Ray Diffraction Data Collected in Oscillation Mode“: Otwinowski, Z.; Minor, W. in Carter, C. W.; Sweet, R. M. (eds.): *Methods in Enzymology, Vol. 276, Macromolecular Crystallography, Part A*, pp. 307–326, Academic Press **1997**.
- [30] SORTAV, Blessing, R. H. *Acta Crystallogr. Sect.* **1995**, A51, 33–38.
- [31] G. M. Sheldrick, *Acta Crystallogr. Sect.* **1990**, A46, 467–473.
- [32] G. M. Sheldrick, *SHELXL-97* (Release 97-2), University of Göttingen, Germany, **1997**.